*Original Russian Text:* Kukudzhanov K.V., Levitin A.L. Deformation processes of elastoplastic material with defects under electrodynamic loading. *PNRPU Mechanics Bulletin*, 2015, no. 1, pp. 106-120. DOI: 10.15593/perm.mech/2015.1.07

**PNRPU MECHANICS BULLETIN**

**№ 1-2, 2018**

http://vestnik.pstu.ru/mechanics/about/inf/

DOI: 10.15593/perm.mech/eng.2018.1.04
UDC 539.3

# DEFORMATION PROCESSES OF ELASTOPLASTIC MATERIAL WITH DEFECTS UNDER ELECTRODYNAMIC LOADING

**K.V. Kukudzhanov, A.L. Levitin**

Ishlinsky Institute for Problems in Mechanics of Russian Academy of Sciences, Moscow, Russian Federation

ARTICLE INFO

Received: 23.05.2016
Accepted: 03.06.2016
Published: 30.06.2018

*Keywords:*

electroplasticity, direct numerical modelling, defective material, electromagnetic field and temperature localization, melting, evaporating

ABSTRACT

The processes occurring in the metallic samples under the impact of electrical current of high density are considered. The processes occurring in the vicinity of microdefects in the form of flat cracks under the action of electric current are studied. The dynamic problem is solved numerically for a representative element of the material with a crack. The problem is solved in two stages using finite elements method. At the first stage, we have studied the thermal electrodynamic problem in order to obtain the temperature distribution and the regions of phase transformations in the material. Regions of the phase transformations (melting and evaporation of the material) are cross-calculated without the explicit allocation of the phase boundaries.At the second stage, we have solved a coupled unsteady thermomechanical problem of deformation of the heated elastoplastic sample taking account of the initial temperature field distribution in the material obtained at the first stage at different moments of time. Additionally, quasistatic thermomechanical problem was solved in order to obtain the displacement field (residual strain) after temperature equalization in the material.

The influence of the size and orientation of microcracks on the localization of the electromagnetic field in the region of the defect is examined. The calculations on the base of the proposed model show that the current density at the tips of the microcracks may by an order exceed the current density applied to the sample. Numerical modelling has shown, that large gradients of electromagnetic field and current arise in the vicinity of the microdefects, which leads to intensive heating, melting and evaporation of the metal in the tips of the microcracks. The melted material flows into the microcrack under the action of thermal stresses. At the same time its evaporation takes place. The shores of the microcracks converge. All these processes lead to a "healing" of defects.



© **Konstantin V. Kukudzhanov** – CSc in Physical and Mathematical Sciences, Senior Research, e-mail: kconstantin@mail.ru

**Alexander L. Levitin** – Junior Research, e-mail: alex_lev@ipmnet.ru

## 1. Introduction

Heating of a sample with the low-density electric current $\mathbf{j} \approx 10\,\mathrm{A/m^2}$ for a long period of time $\tau \approx 10^3\,\mathrm{s}$ is one of best studied and applicable methods of processing metals and alloys. This kind of effect leads to an overall (integral) material heating, a decrease of absolute values of its mechanical characteristics, and makes it easier to perform the tooling of a heated sample. At the same time, if we intensify the action of the electromagnetic field on the conducting material and make this action short, expose it to the current density of $\mathbf{j} \approx 10^9\,\mathrm{A/m^2}$ and $\tau \approx 10^{-4}\,\mathrm{s}$ time, it can significantly improve plastic properties of a material by incresing its plastic deformations under fracture (from tens to hundreds of percent for different materials and alloys [1-2, 5, 7, 8-11]). This effect was called the electroplastic effect. Despite the fact that this effect is widely used in industry, still there is no consensus on the nature of this effect, and the discussion about its fundamental principles and physical mechanism are still running. Its critical distinction is the increase of the ultimate plastic deformation by means of other mechanisms of electromagnetic field effects, if we compare it with the integral heating [14-15, 18-19]. Meanwhile the material retains its plastic properties over the entire period of time after the current exposure is finished (the effect has a lasting residual character), which makes it possible to use this effect in manufacturing processes, both for simultaneous and subsequent electromechanical effects.

One of explanations of the electroplastic effect is the hypothesis about the rearrangement (change) of the defects system in a material under the effect of the electromagnetic field [3, 12-15]. The works of [12, 13] present the theoretical studies aiming to explain this effect. They show that the body with defects in the form of disklike cracks at a stationary field of temperatures (which occurs after the action of the electric current) undergoes a partial closure of cuts (cracks). The works in [14-17] contain the results obtained for the nonstationary field of temperature with the closure of defects in the form of cuts, as well as the distribution of compressive plastic stresses, which lead to a partial "healing" of cylinder defects. The works in [18-19] offer a quasistatic model of the material thermoelectroplastic deformation, and the numerical method of solving the resulted system of equations, which became the basis for solving the deformation and fracture problems of the material's representative elements containing both single meso- and macrodefects, as well as their ordered set in the form of flat cracks and cylinder pores under different modes of electrodynamic and thermomechanical loadings. It is shown that an inhomogeneous temperature field with temperature localization arises in the sample under the action of an electric current near macrocracks and pores, localizing the temperature, which reaches the melting point at their vertices (tips), and as a result, leads to melting the material and "collapsing" defects, such as cuts and flat cracks. Formation of pores leads to a decrease of the conventional yield limit and increase of ultimate plastic deformation.

The present work is a continuation of the cycle of works [18-21], it is devoted to studying the processes occurring in the vicinity of microdefects of a material when metal specimens are subjected to electric current. The model proposed in [18-19] is developed here with the aim of investigating dynamic processes occurring at the level of microdefects at small times of an electromagnetic field exposure to the material ($\tau \approx 10^{-4}\,\mathrm{s}$), taking into account its phase transformations. We solve the problem of the short-term action of the electromagnetic field on flat microcracks on the basis of the created model. The changes in electromagnetic, temperature fields, phase transitions and stress-strain state in the neighbourhood of microcracks within time are studied. By understanding these processes, it will become possible to have a clear mechanism of the electroplastic effect in terms of the hypothesis of a rearrangement in the material's structure of defects, to come closer to the explanation of the experimentally observed changes of the thermomechanical material properties and use the obtained modelling results in order to develop new methods of material processing.

## 2. Problem Setting

A conductive material with an ordered defect structure is considered, which consists of periodically distributed representative elements, as shown in Fig. 1, containing the defects such as flat microcracks. The material is under the effect of a short-pulse high-energy electromagnetic field of a certain intensity (the current density is from $10^8$ to $10^{11}$ A/m$^2$) and the duration (up to 100 microseconds). In this case, the task is to investigate in time the processes of changing the electric and temperature fields in the material, and their effect on phase transformations and the stress-strain state in the vicinity of microdefects. In order to solve this task, it is proposed to use the dynamic model of interaction between the electromagnetic and temperature fields on the pre-damaged material with defects. The model describes this process stepwise. This problem was solved using the finite element method in two time stages.

At the first stage, we solve the electrothermal problem for representative elements (volumes) of the material with defects in the form of flat cracks, in order to get fields of electric potential, density of current and temperature in the sample depending on time. The first stage finishes, when the action of the electromagnetic field on the material is over.

At the second stage, at the same region of integration, we solve the thermomechanical problem with the initial destribution of the temperatures field in the material, which has been obtained at the first stage. The main target at the second stage is getting the fields of displacements,

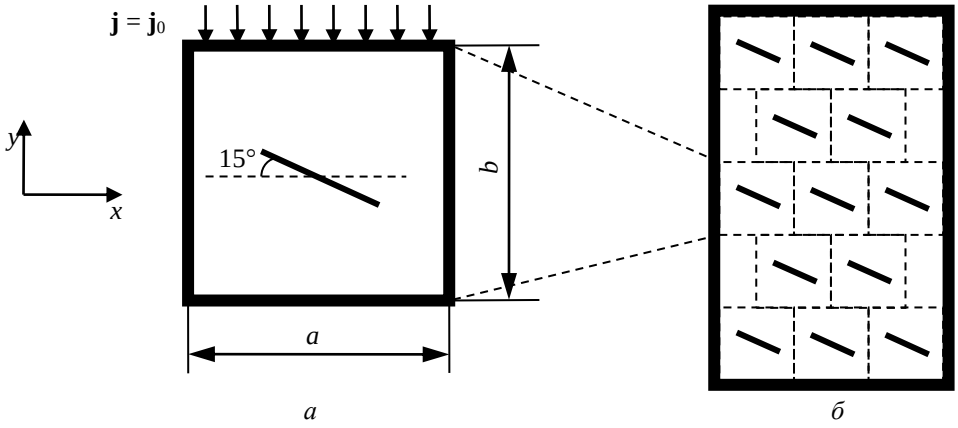


Fig. 1. A representative element (*a*) and an ordered structure of defects (*b*)

velocities and stresses in the sample during and after the electromagnetic effect, as well as the field of temperature. In this case, both the temperature fields at various times before the end of the action of the electric current on the material, as well as the temperature field formed in the material at the time of the end of the current action were used as the initial temperature field for modelling. Additionally, the thermomechanical problem was solved in the quasistatic setting, in order to obtain the displacement field (residual deformations) after the temperature equalization in the material.

This problem setting is explained by physically splitting the complex phenomenon into separate processes (electrothermal and thermomechanical) due to a short-term effect of the electromagnetic field on the material, as well as by the complexity of a simultaneous solution of equations of the coupled electrothermoplasticity, also because of limitations of computer time

## 3. Main Equations of the Electrothermomechanical Model

To calculate the electric potential and temperature in the conductive material at the first stage, we use the charge conservation law in combination with the Ohm's law in the following form:

$$\int_S \mathbf{j}\cdot\mathbf{n}\,dS = \int_V r_c dV, \tag{1}$$

$$\mathbf{j} = \sigma^E \mathbf{E} = -\sigma^E \frac{\partial \varphi}{\partial \mathbf{x}} \tag{2}$$

$\sigma^E(T)$ where $V$ is the arbitrary volume with the surface $S$; $\mathbf{n}$ is the external normal to $S$; $\mathbf{j}$ is the current density and $r_c$ is the inner volume source of current per unit volume, $\mathbf{E}(x)$ is the intensity of the electric field, determined as a negative gradient of the electric potential $\mathbf{E} = -\partial\varphi/\partial x$, $\varphi$ is the electric potential, $\sigma^E(T)$ is the matrix of conductivity, $T$ is temperature.

Based on (1) and (2) equations, we get the main equation of the finite element model in a variation form:

$$\int_V \frac{\partial \delta\varphi}{\partial \mathbf{x}}\,\sigma^E\,\frac{\partial \varphi}{\partial \mathbf{x}}\,dV = \int_S \delta\varphi\; j\; dS + \int_V \delta\varphi\; r_c\; dV, \tag{3}$$

where $j = -\mathbf{j}\cdot\mathbf{n}$ is the current density, integrated along the surface $S$; $\delta\varphi$ are the variations of the electric potential.

To get the temperature field at the first and second stages, we use the energy conservation law:

$$\int_V \rho \dot{U}\, dV = \int_S q dS + \int_V r dV, \tag{4}$$

where $\rho$ is density, $\dot{U}$ is the material derivative of the internal energy, q is the energy flow through the surface per unit area and r is the heat energy in a unit volume in the current configuration of the body.

The heat flow **f** is determined by Fourier's law

$$\mathbf{f} = -\mathbf{k}\frac{\partial T}{\partial \mathbf{x}} \tag{5}$$

where $\mathbf{k} = \mathbf{k}(T)$ is the matrix of the material heat conductivity .

The variational formulation of the energy equation (4) is used in a weak form of Bubnov-Galerkin method:

$$\int_V \rho \dot{U}\,\delta T\, dV + \int_V \frac{\partial \delta T}{\partial \mathbf{x}}\cdot\mathbf{k}\cdot\frac{\partial T}{\partial \mathbf{x}}\,dV = \int_V \delta T\, r\, dV + \int_{S_q} \delta T\, q\, dS, \tag{6}$$

where $\delta T$ are the variations of temperature fields satisfying the boundary conditions of periodic behavior.

When modelling, the Joule-Lenz's law is considered, which describes the intensity of the electric energy dissipated by the current running along the conductor:

$$P_E = \mathbf{j}\cdot\mathbf{E} = \frac{\partial \varphi}{\partial \mathbf{x}}\cdot\sigma^E\cdot\frac{\partial \varphi}{\partial \mathbf{x}}. \tag{7}$$

The amount of the electric energy released in the form of inner heat is equal to

$$r = \eta P_E, \tag{8}$$

where η is the corresponding Taylor-Kuni coefficient of transformation of electric energy into the heat energy.

The amount of the electric energy released on the body's surface, has the following form

$$q_E = f\eta_g P_E, \tag{9}$$

where $\eta_g$ is the surface coefficient of energy transformation into the thermal energy, f determines the complete destribution of heat between external surfaces.

The pulse balance equation in the variational formulation takes the following form

$$\int_V \rho\ddot{\mathbf{u}}\,\delta\mathbf{u}\,dV = \int_V \boldsymbol{\sigma}\,\delta\boldsymbol{\varepsilon}\,dV - \int_V \rho\mathbf{b}\,\delta\mathbf{u}\,dV - \int_S \mathbf{t}\,\delta\mathbf{u}\,dS, \tag{10}$$

where u is the vector of displacements, σ is the stress tensor, ε is the tensor of complete deformations, b is the vector of bulk (mass) forces, t is the vector of surface forces, $\delta\mathbf{u}$ and δε is the variation of displacements and corresponding total deformations.

After using the finite element approximation of type $\mathbf{u}(\mathbf{x},t) = [N(\mathbf{x})]\{U(t)\}$ (here $\{U(t)\}$ is the vector of nodal displacements, $[N(\mathbf{x})]$ is the shape function matrix ) (10) can be shown in the following form:

$$[M]\{\ddot{U}\} + [K^{\text{ep}}]\{U\} = \{F\}, \tag{11}$$

where $[M] = \int_V [N]^{\text{T}}[N]\rho\,dV$ is the mass matrix, $\{F\} = \int_V [N]^{\text{T}}\rho\mathbf{b}\,dV + \int_S [N]^{\text{T}}\mathbf{t}\,dS$ $\{\boldsymbol{F}\}$ is the vector of forces acting on the body's nodes, [B(**x**)] is the matrix of gradients, $[D^{\text{ep}}]$ are tangential modules of the elastoplastic body.

The central difference approximation in respect with time is used according to the Lax-Wendroff-type scheme:

$$\begin{aligned} \dot{\mathbf{U}}^{(n+1/2)} &= \dot{\mathbf{U}}^{(n-1/2)} + \frac{\Delta t^{(n+1)} + \Delta t^{(n)}}{2}\ddot{\mathbf{U}}^{(n)} \\ \mathbf{U}^{(n+1)} &= \mathbf{U}^{(n)} + \Delta t^{(n+1)}\dot{\mathbf{U}}^{(n+1/2)} \\ \ddot{\mathbf{U}}^{(n)} &= [M]^{-1}\left(\{F\} - [K^{\text{ep}}]\{U\}\right) \end{aligned} \tag{12}$$

at the initial step, the initial nodal velocities $\dot{\mathbf{U}}^{(0)}$ are known, thus we get $\dot{\mathbf{U}}^{(-1/2)} = \dot{\mathbf{U}}^{(0)} - \frac{\Delta t^{(1)}}{2}\ddot{\mathbf{U}}^{(0)}$.

The calculations were made using the software called ASTRA, which has been developed at the Modelling Laboratory of the Ishlinsky Institute for Problems in Mechanics of Russian Academy of Sciences headed by Prof. N.G. Burago. The presented calculations were carried out in a two-dimensional setting using linear four-nodal isoparametric finite elements.

The strain rate tensor of the thermoelastoplastic material is equal to

$$\dot{\boldsymbol{\varepsilon}} = \dot{\boldsymbol{\varepsilon}}^{\text{el}} + \dot{\boldsymbol{\varepsilon}}^{\text{pl}} + \dot{\boldsymbol{\varepsilon}}^{\text{th}}, \tag{13}$$

where $\dot{\boldsymbol{\varepsilon}}^{\text{el}}$, $\dot{\boldsymbol{\varepsilon}}^{\text{pl}}$, $\dot{\boldsymbol{\varepsilon}}^{\text{th}}$ are the strain rate tensors of elastic, plastic and thermal deformations. The thermal deformation in a differential form will be as follows

$$d\varepsilon^{\text{th}} = \alpha(T)\,dT, \tag{14}$$

where α is the thermal expansion coefficient.

For elastic and plastic deformations, we take the the Hook's law and the associated flow rule with the Mises yield criterion respectively

$$\boldsymbol{\sigma} = \lambda\boldsymbol{\varepsilon} : \mathbf{I} + 2\mu\left(\boldsymbol{\varepsilon} - \boldsymbol{\varepsilon}^{\text{pl}}\right),\ \dot{\boldsymbol{\varepsilon}}^{\text{pl}} = \dot{\Lambda}\,\mathbf{s},\ \ \bar{\sigma} = \sigma_Y,\ \ \bar{\sigma} = \sqrt{\tfrac{3}{2}\mathbf{s} : \mathbf{s}}, \tag{15}$$

where $\sigma_Y = \sigma_Y(T)$ is yield stress, **s** is the deviator of tensor of stresses.

Thermal energy per unit volume in the current configuration of the body due to the dissipation of plastic deformation is taken as follows:

$$r = \eta\boldsymbol{\sigma} : \dot{\boldsymbol{\varepsilon}}^{\text{pl}}, \tag{16}$$

where η is the share of inelastic energy, which is spent on heat formation, $\dot{\boldsymbol{\varepsilon}}^{\text{pl}}$ is the strain rate tensor of plastic deformation.

Equations (3), (6)–(9), (16) form complete simultaneous equations of the electrothermal problem. Equations (6)–(10), (13)–(16) form a complete system of equations of the thermomechanical problem.

In the proposed model, the connection of problems (electric and thermal, mechanical and thermal) was also considered by the dependences of all the physical and mechanical characteristics of the material (density, specific thermal capacity, conductivity, coefficient of thermal expansion, elastic moduli, yield stress etc.) on temperature.

As the time of the electromagnetic effect on the material doesn't exceed $10^{-4}$ c, at the first stage we will solve the problem in the adiabatic approximation.

At the boundary of the integration domain the following conditions are taken for the electrothermal problem: at the boundaries $y = 0$, $y = b$ we set the current density (or the difference of electric potentials) to be constant with respect to $x$, as well as the condition of zero heat flow in the boundary tangent direction; at the boundaries $x = 0$, $x = a$ the current density and the heat flow along the normal to the boundary were considered to be zero. The initial temperature was considered to be constant (0 °C), and the potential was considered to be zero.

When solving the thermomechanical problem, the initial distribution of temperature in the representative element was taken from the solution of the electrothermal problem, and the initial values of the displacement field were considered to be zero. For temperature, the boundary conditions were set the same, as in the electrothermal problem. For the displacements we set the condition of symmetry at $y = 0$, $y = b$, and the periodic boundary condition at $x = 0$, $x = a$.

## 4. Phase Transitions of Material

Regions of the phase transformations (melting and evaporation of the material) are cross-calculated without the explicit allocation of the phase boundaries.

It was considered that the material melted, when the temperature in the nod was $T > T_{\text{melt}}$, where $T_{\text{melt}}$ is the temperature of the material melting. In the nodes, where material melted, there was an abrupt change in all physical properties of the material: conductivity, heat capacity, density, estimated coefficient of linear expansion and all other mechanical characteristics of the material. Such a variation of material properties corresponds with the available experimental data [24–26]. Fig. 2 shows the data about the changes of some of those characteristics versus temperature for zinc.

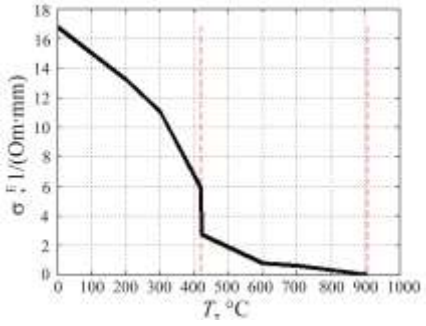


*a*

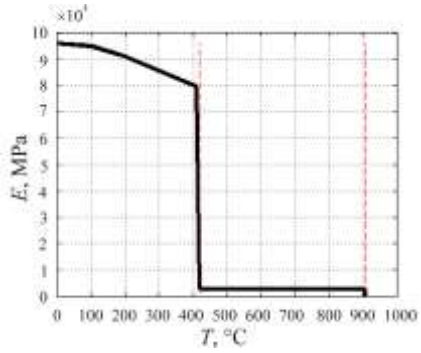


*b*

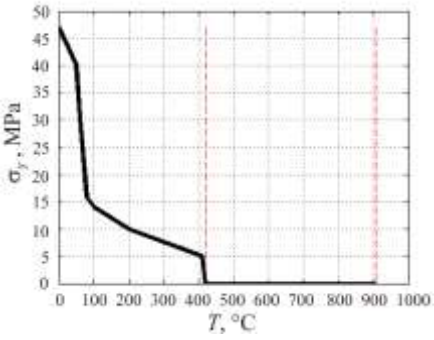


*c*

Fig. 2. The relations of (*a*) conductivity $\sigma^{E}$, (*b*) Young's modulus *E*, (*c*) yield stress $\sigma_Y$ on the temperature *T* (vertical dashed lines indicate the melting point – $T_{\text{melt}}$ = 419 °C and evaporations – $T_{\text{evap}}$ = 906 °C).

Thus, within the proposed model, when reaching the melting point, the material will not loose the ability to conduct electric current (Fig. 2 *a*)б and there comes further heating of the melt. Decreasing of the elastic moduli and yield stress which take place during these processes (Fig. 2 *b*, *c*) makes it possible to describe the further behavior of the material using equations in (15) and perform the cross-calculation without changing the numerical scheme.

It is considered that the material evaporated, when the temperature in the node reached $T > T_{\text{evap}}$, where $T_{\text{evap}}$ is the temperature of the material evaporation. Wheras in the nodes where the material evaporated, it was considered that the current density was $j = 0$, the temperature was $T = T_{\text{evap}}$, and the stress tensor was $\boldsymbol{\sigma} = 0$.

Thus, within the proposed model, when reaching the melting point, the material looses the ability to conduct electric current, and there comes no further heating of it. It is considered that metal evaporation into the crack occures with the same speed as for vacuum which equals the speed of sound. Meanwhile it looses the properties of a viscous fluid, and it is modelled with a low-pressure gas.

## 5. Results of Numerical Modelling

All the calculations were carried out for the case of plane deformation. The current density or difference of electric potentials at the boundary of the representative element was constant over the entire period of the electromagnetic pulse.

When the electric current penetrates the sample with defects (Fig. 1), in the vicinity of defects in the form of flat cracks or cylinder pores, there come large gradients of electric potential which lead to abrupt changes of the current density field, including a significant increase of the current density in the neighbourhood of peaks (tips) of cracks or pore edges, compared to the current density supplied to the sample. Let us note that the current density in the sample without defects is constant at a distance of the same order with the characteristic sizes of the representative element, and it is equal to the density of the applied current. The increase of the current density at the tips of the meso- and macrocracks or pores' edges, in its turn, leads to a strong local heating [18–21].

For microcracks sized about 10 microns, the calculations according to the proposed model show that the current density at the tips may by an order exceed the density of the current applied to the sample. Fig. 3a shows the dependence of the maximal current density *j* (А/мм$^2$) at the tip of the flat microcrack with a rounded tip on its length *l* micron in the sample made from zinc under the current pulse of $1.5 \cdot 10^2$ A/mm$^2$. The distance between the shores and the the radius of curvature at the tip of the microcracks was такет to be 1 micron. Wheras the number of defects in the sample was meant to be constant. Let us note that the maximum current density at the tip of the crack is also by an order of magnitude higher than the current density in the

sample, which is calculated for a decreased sectional area of the sample caused by microcracks. It indicates a significant nonhomogeneity of the field of the current density, and, thus, the temperature in the sample with microcracks.

The diagram shows that the microcracks's size is by an order of magnitude larger, and leads to a decrease of the maximum current density in its tip only by 2.8 times.

Fig. 3a shows the dependence of the maximum current density $j$ (A/mm$^2$) at the upper tip of the flat microcrack with a length of 50 microns on the tilting angle of the crack plane towards the $x$ axis in the zinc specimen under the current pulse of $1.5 \cdot 10^2$ A/mm$^2$. The distance between the shores and the the radius of curvature at the tip of the microcracks was take to be 1 micron. The diagram shows that the maximum current density at the tip of the crack remains almost constant in the range of angles 0°–15°. When the angle is further increased, the maximum current density at the tip of the crack decreases nonlinearly. Nevertheless, this decline is insignificant (less than 25 %), when the angle changes in quite a wide range of angles covering most probable angles of defects formation under a preliminary plastic deformation of metal before the material processing with electric current (this deformation occurs in the direction of the electric current along the axis $y$ or $\alpha = 90°$).

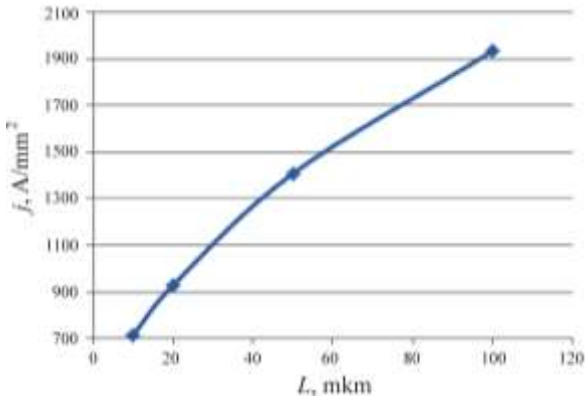


*a*

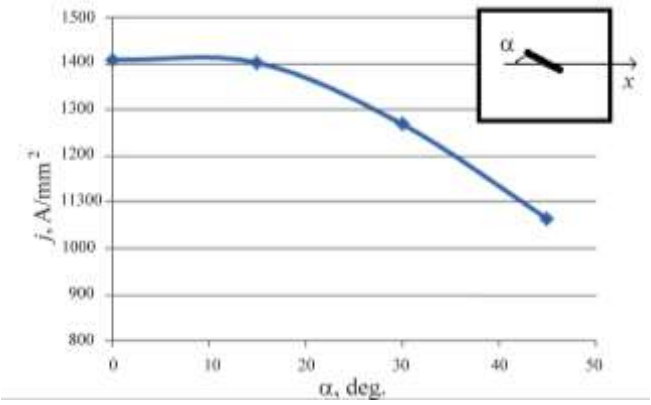


*b*

Fig. 3. The current density with respect to the microcrack length (*a*) and its slope (*b*)

Fig. 4 shows (*a*) the fields of current density and (*b*) temperature (at the time $t = 37.5$ microseconds) in the neighbourhood of the tip of the microcracks with the length of 50 microns with the tilt angle to the axis $x$ which is equal to 15° for the sample made from zinc, affected by the pulse amounting to $7.3 \cdot 10^3$ A/mm$^2$ and lasting for 50 microseconds. The sizes of the representative element are $a$ = 400 micron, $b$ = 375 micron.

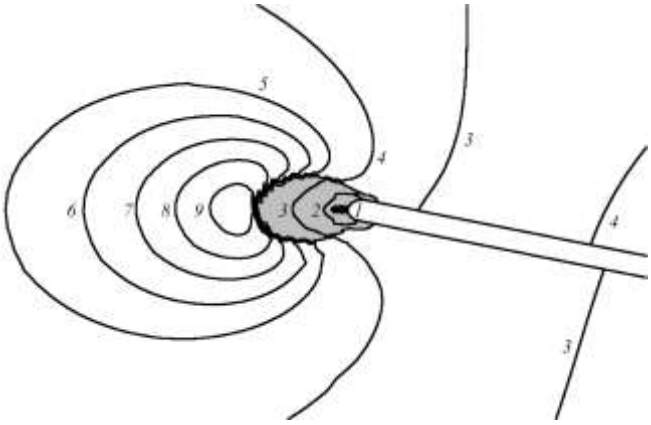


*1* – 0, *2* – 3000, *3* – 6000, *4* – 9000, *5* – 12000, *6* – 13500, *7* – 15000, *8* – 16500, *9* – 18000

*a*

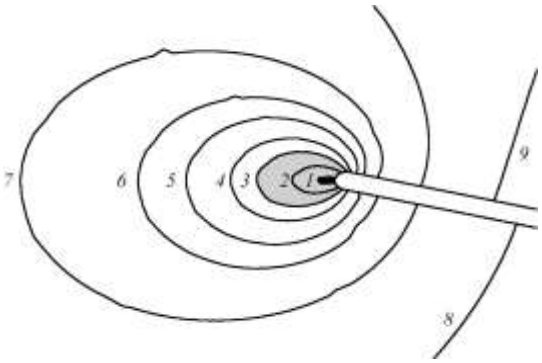


*1* – 906, *2* – 600, *3* – 419, *4* – 300, *5* – 200, *6* – 150, *7* – 100, *8* – 50, *9* – 20

*b*

Fig. 4. Isolines of (*a*) current A/m$^2$ and (*b*) temperature °C at $t$ = 37,5 microseconds, the black area is the evaporation region, the grey area is the melting region

As a result of modelling, it was revealed that at the shores of the microcrack, there are regions (at the distance of 18 micron from the crack tip), where the current density amounts to only 30 A/mm$^2$, i.e. more than 100 times less, than the density of the applied current. Meanwhile, in the region of the microcrack's tips, the electric current density is by an order of magnitude higher, than the applied electric current. So, large gradients of electromagnetic field occuring as a result of the effect in the neighbourhood of microdefects change the current density at microdistances by 1000 and more times. This circumstance leads to a fast

growth of temperature and material melting. In Fig. 4. the zones where the meaterial melted are well seen at the tips of the crack.

However, the fields occurring under the electro-magnetic action of the field of current and temperature at the tip of the crack quite quickly lead not only to melting, but also to evaporation of the material. Fig. 5 shows the dependences of the maximum current density ($j$ (A/mm$^2$) and temperature $T$ (°C) at the upper tip of the microcrack with the length of 50 micron on time $t$ microseconds. It is seen from the diagrams, that the maximum current density at the tip of the crack declines with the growth of temperature; and at instant of time $t$ = 6 microseconds, the temperature reaches the value of $T_{melt}$ = 419 °C, after which the material starts to melt, which is accompanied by an abrupt decline of the current density. The further decline of the current density and incline of temperature get slower, but already at the instant of time $t$ = 28 microseconds, the temperature at the tip of the microcrack reaches its critical value ($T_{evap}$ = 906 °C), and an intensive evaporation of the material starts, with its transfer into the defect. In Fig. 4 the zones where the material evaporated are well seen at the tips of the crack.

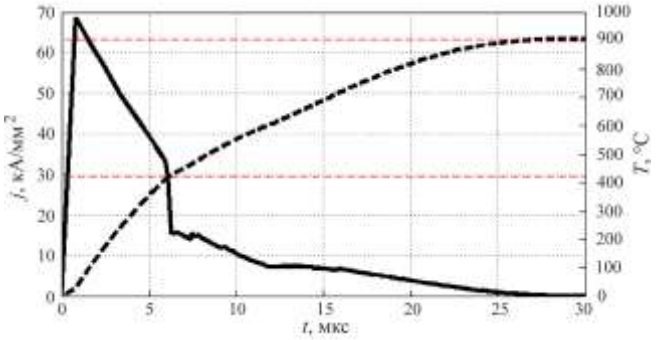


Fig. 5. The dependence of the current density, kA/mm$^2$ (a solid line) and temperature $T$, °C (dashed line) at the tip of the crack versus time in microseconds (horizontal dashed lines show the temperature of melting $T_{melt}$ = 419 °C and evaporation $T_{evap}$ = 906 °C)

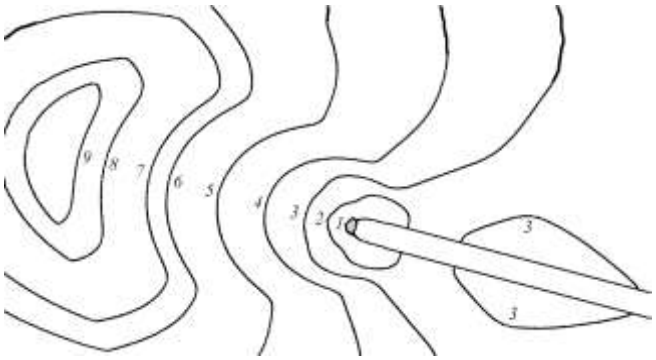

Fig. 6. The pressure at the upper tip of the crack $t$ = 6.25 microseconds (grey colour shows the tensile region, *1* – 0, *2* – 15, *3* – 25, *4* – 40, *5* – 60, *6* – 75, *7* – 80, *8* – 90, *9* – 95° MPa)

Meanwhile it is necessary to note that the action of the intensive current, fast heating and melting of the material, accompanied with its thermal expansion, lead to high concentrations of stresses in the neighbourhood of the microcracks' tips, and, as a consequence, the outflow of the melted material into the crack. Fig. 6. shows the field of hydrostatic pressure (MPa) at the tip of the crack after 6.6 microseconds after the electric current affects the specimen (uniform extension has the opposite sign).

Within time a further fusion of the tips of the crack, outflow of the melted material into the microcracks released with its evaporation. Fig. 7 presents the field of temperature in the vicinity of the microcrack after the current's action stops (instant of time $t$ = 50 microseconds). The regions, where melting and evaporation of the material took place, reach the sizes of several microns.

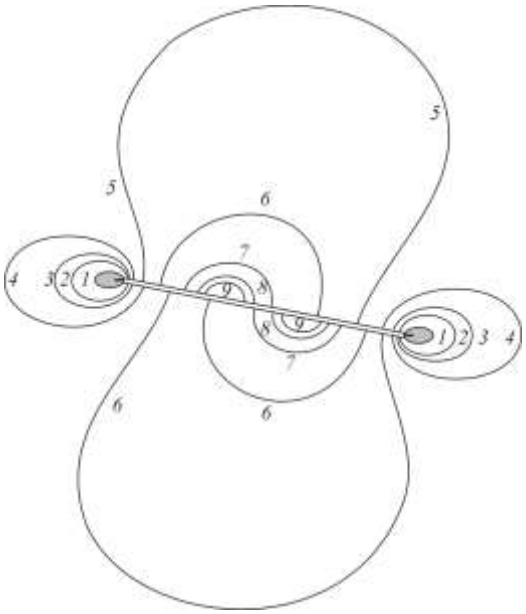

Fig. 7. Isolines of temperature at the instant of time $t$ = 50 microsecond (a black part shows the evaporation region, the grey part shows the melting region, *1* – 419, 2 – 300, *3* – 200, *4* – 100, *5* – 50, *6* – 20, *7* – 5, *8* – 2, *9* – 1 °C)

The calculations demonstrate that both over the entire period of electric current's action, as well as after it finishes up to the temperature equalization, the shores of the microcrack are displaced towards each other throughout the length of the microcrack under compressive temperatures stresses (the effect of defects "healing"). It complies well with the analytical solutions, described in [12-17] and numerical ones in [18-19] for cuts and pores, obtained in the quasistatic setting. The performed modelling of a short-term effect by the intensive electric current on the tilted microcrack proves the preservation of the microdefects "healing" effect in a nonstationary waveform setting of the problem. The solidification of the melt in the microcrack and the condensation of metal vapors on its shores enhance this effect.

The work is supported by the Russian Foundation for Basic Research (Grant Nr.12-01-00807).

## References


1. Spitsyn V.I., Troitskii O.A. Elektroplasticheskaia deformatsiia metallov [Electroplastic deformation of metals]. Moscow, Nauka, 1985, 160 p.

2. Beklemishev N.N., Kukudzhanov V.N., Porokhov V.A. et al. Plastichnost' i prochnost' metallicheskikh materialov s uchetom impul'snogo vozdeistviia vysokoenergeticheskogo elektromagnitnogo polia [Plasticity and strength of metallic materials with the pulse action of a high-energy electromagnetic field taken into account]. Preprint No. 372, IPM AN SSSR, Moscow, 1989, 56 p.

3. Beklemishev N.N., Koryagin N.I., Shapiro G.S. Influence of Locally Inhomogeneous Pulse Electric Field on Plasticity and Strength of Conducting Materials, *Russ. Metallurgy (Metally)*, 1984, No. 4, pp. 184-187.

4. Kravchenko V.Ya. Effect of a Directed Electron Beam on Moving Dislocations, *Sov. Phys. JETP*, 1967, Vol. 24, No. 6, pp. 1135-1142.

5. Klimov K.M., Novikov I.I. Influence of Temperature Gradient and Electric Current of High Density on Plastic Strain under Tension of Metallic Wires, *Russ. Metallurgy (Metally)*, 1978, No. 6, pp. 175-180.

6. Finkel' V.M., Golovin Yu.I., Sletkov A.A. Possibility of Braking Rapid Cracks by Pulses of Current, *Sov. Phys. Dokl.*, 1976, Vol. 21, No. 4, pp. 216.

7. Conrad H. Electroplasticity in metals and ceramics, *Materials Science and Engineering: A.*, 2000, Vol. 287, No. 2, pp. 276-287. DOI: 10.1016/S0921-5093(00)00786-3

8. Stepanov G.V., Babutskii A.I., Mameev I.A. High-Density Pulse Current-Induced Unsteady Stress-Strain State in a Long Rod, *Strength of Materials*, 2004, Vol. 36, No. 4, pp. 377-381. DOI: 10.1023/B:STOM.0000041538.10830.34

9. Dubinko V.I., Klepikov V.F. Kinetic Mechanism of the Electroplastic Effect in Metals, *Bull. Russ. Acad. Sci. Phys.*, 2008, Vol. 72, No. 9, pp. 1188-1189. DOI: 10.3103/S1062873808090037

10. Stashenko V.I., Troitskii O.A., Novikova N.N., Electroplastic Drawing of a Cast-Iron Wire, *J. Machinery Manufact. Reliabil.*, 2009. Vol. 38, No. 2, pp. 182-184. DOI: 10.3103/S1052618809020149

11. Troitsky O.A. Use of Electroplastic Effect in Metal Forming, *Metallurg. Mashinostr.*, 2010, No. 4, pp. 45-48.

12. Salganik R.L. Thermoelastic Equilibrium of a Solid with Cracks under Heating Caused by Passage of a Current Perpendicular to the Cracks, *Mech. Solids*, 1978, Vol. 13, No. 5, pp. 129-138.

13. Salganik R.L., Heating of a Material with an Ellipsoidal Nonuniformity as a Result of Electrical Losses, *Mech. Solids*, 1980, Vol. 15, No. 6, pp. 87-98.

14. Klyushnikov V.D., Ovchinnikov I.V., Plane Problem of Effect of an Instantaneous Point Heat Source, *Mech. Solids*, 1988, Vol. 23, No. 4, pp. 113-117.

15. Ovchinnikov I.V. Vliianie vozdeistviia elektrotoka na plastichnost' metallov [Influence of Electric Current Action on Plasticity of Metals]. PhD's Dissertation in Mathematics and Physics, Moscow, 1969. 123 p.

16. Kukudzhanov V.N., Beklemishev N.N., Porokhov V.A. Kvazistaticheskoe odnoosnoe razuprochnenie nekotorykh metallicheskikh materialov v usloviiakh zhestkogo zakrepleniia pod deistviem elektromagnitnogo polia [Quasistatic Uniaxial Softening of Some Metallic Materials under Conditions of Rigid Fixation and under Action of Electromagnetic Field], *Vestnik Nizhegorod. Univ. Ser. Mekh.*, 2003, No. 1 (5), pp. 129-141.

17. Porokhov V.A., Kukudzhanov V.N. Nekotorye osobennosti vliianiia impul'sov toka na plastichnost' metallov pri vysokikh skorostiakh deformatsii [Some Characteristic Features of the Influence of Current Pulses on the Metal Plasticity at High Strain Rates], *Probl. Prochn. Plastichn.*, 2005, No. 67, pp. 132-142.

18. Kukudzhanov V.N., Kolomiets-Romanenko A.V. Study of the Influence of Electric Current Dynamical Action on Mechanical Properties of Materials with Ordered Structure of Defects, *Mech. Solids.*, 2010, Vol. 45 No. 3, pp. 465-475. DOI: 10.3103/S0025654410030167

19. Kukudzhanov V.N., Kolomiets-Romanenko A.V. A Model of Thermoelectroplasticity of Variations in the Mechanical Properties of Metals Based on Defect Structure Reorganization under the Action of Pulse Electric Current, *Mech. Solids.*, 2011, Vol. 46, No. 6, pp. 814-827. DOI: 10.3103/S0025654411060021

20. Kolomiets A.V., Kukudzhanov V.N., Kukudzhanov K.V. O perekhode neodnorodnykh uprugoplasticheskikh materialov s defektami v makrorazrushennoe sostoianie [About transition of inhomogeneous elastic-plastic materials with defects into the macrofracture state]. Preprint No. 1053, IPMech RAS, Moscow, 2013, 42 p.

21. Kolomiets A.V., Kukudzhanov V.N., Kukudzhanov K.V., Levitin A.L. Modelirovanie neuprugogo razrusheniia neodnorodnykh materialov pri elektrodinamicheskom i termomekhanicheskom vozdeistviiakh [Modeling of the inelastic fracture of heterogeneous materials under electrodynamic and thermomechanical loading]. Preprint No. 1054, IPMech RAS, Moscow, 2013, 35 p.

22. Xiaoxin Ye, Yanyang Yang, Guolin Song, Guoyi Tang. Enhancement of ductility, weakening of anisotropy behavior and local recrystallization in cold-rolled Ti-6Al-4V alloy strips by high-density electropulsing treatment, *Appl. Phys. A.*, 2014, Vol. 117, No. 4, pp. 2251-2264. DOI: 10.1007/s00339-014-8655-1

23. Min-Sung Kim, Nguyen Thai Vinh, Hyeong-Ho Yu, Sung-Tae Hong, Hyun-Woo Lee, Moon-Jo Kim, Heung Nam Han, and John T. Roth. Effect of Electric Current Density on the Mechanical Property of Advanced High Strength Steels under Quasi-Static Tensile Loads. *International Journal of Precision Engineering and Manufacturing*, 2014, Vol. 15, No. 6, pp. 1207-1213. DOI: 10.1007/s12541-014-0458-y

24. Gavrilin I.V. Plavlenie i kristallizatsiia metallov i splavov [Melting and crystallization of metals and alloys]. Vladimir, Vladimir State University, 2000. 260 p.

25. Pikunov M.V. Metallurgiia rasplavov. Kurs lektsii. [Metallurgy of the melts. A course of lectures]. Moscow: MISiS, 2005. 286 p.

26. Pikunov M.V. Plavka metallov. Kristallizatsiia splavov. Zatverdevanie otlivok. [Metal melting. Alloy crystallization. The solidification of castings]. Moscow: MISiS, 1997. 374 p.